Wan, Xingbang; Shi, Junjie; Klemettinen, Lassi; Chen, Min; Taskinen, Pekka; Jokilaakso, Ari

Equilibrium phase relations of CaO–SiO2–TiO2 system at 1400°C and oxygen partial pressure of 10−10atm

Published in:
Journal of Alloys and Compounds

DOI:
10.1016/j.jallcom.2020.156472

Published: 20/12/2020

Document Version
Peer-reviewed accepted author manuscript, also known as Final accepted manuscript or Post-print

Journal Pre-proof

Equilibrium phase relations of CaO–SiO_2–TiO_2 system at 1400□°C and oxygen partia

pressure of 10^{-10}□atm

Xingbang Wan, Junjie Shi, Lassi Klemettinen, Min Chen, Pekka Taskinen, Ari Jokilaakso

PII: S0925-8388(20)32836-X

DOI: https://doi.org/10.1016/j.jallcom.2020.156472

Reference: JALCOM 156472

To appear in: *Journal of Alloys and Compounds*

Received Date: 27 May 2020

Revised Date: 19 July 2020

Accepted Date: 20 July 2020

Please cite this article as: X. Wan, J. Shi, L. Klemettinen, M. Chen, P. Taskinen, A. Jokilaakso, Equilibrium phase relations of CaO–SiO_2–TiO_2 system at 1400□°C and oxygen partial pressure of 10^{-10}□atm, *Journal of Alloys and Compounds* (2020), doi: https://doi.org/10.1016/j.jallcom.2020.156472.

Xingbang Wan: Investigation; Methodology; Writing - original draft.

Junjie Shi: Investigation; Conceptualization; Data curation; Writing - original draft; Software.

Lassi Klemettinen: Methodology; Writing - review & editing.

Min Chen: Methodology; Writing - review & editing.

Pekka Taskinen: Software; Supervision; Writing - review & editing.

Ari Jokilaakso: Project administration; Resources; Validation; Writing - review & editing; Funding acquisition.

Equilibrium phase relations of $CaO-SiO_2-TiO_2$ system at 1400 °C and oxygen partial pressure of 10^{-10} atm

Xingbang Wan[1], Junjie Shi[1,*], Lassi Klemettinen[1], Min Chen[1], Pekka Taskinen[1], Ari Jokilaakso[1]

Affiliation:

[1] Department of Chemical and Metallurgical Engineering, School of Chemical Engineering, Aalto University, PO Box 16100, FI-00076 Aalto, Finland.

*Corresponding author.

Emails for authors:

Xingbang Wan: xingbang.wan@aalto.fi

Junjie Shi: junjieshi@126.com

Lassi Klemettinen, lassi.klemettinen@aalto.fi

Min Chen, min.chen@aalto.fi

Pekka Taskinen, pekka.taskinen@aalto.fi

Ari Jokilaakso, ari.jokilaakso@aalto.fi

ORCID

Xingbang Wan, 0000-0001-8378-7600

Junjie Shi, 0000-0002-8673-0404

Lassi Klemettinen, 0000-0001-9633-7131

Min Chen, 0000-0003-0544-4359

Pekka Taskinen, 0000-0001-8332-6230

Ari Jokilaakso, 0000-0003-0582-7181

Abstract: The equilibrium phase relations and liquidus contours for the TiO_x-containing oxide system in reducing atmospheres are of importance in understanding the smelting process of Ti-containing resources. Equilibrium - quenching experiments were conducted at 1400 °C for the $CaO-SiO_2-TiO_x$ system at oxygen partial pressure of 10^{-10} atm controlled by a CO/CO_2 gas mixture. The equilibrium phase compositions were analyzed by scanning electron microscopy - energy dispersive X-ray spectrometry. Perovskite, wollastonite, rutile, and silica were found to coexist with liquid oxide. The 1400 °C isotherm was then constructed for the $CaO-SiO_2-TiO_x$ system, and the results revealed that lower oxygen partial pressures led to shrinkage of the rutile and wollastonite primary phase areas. The comparisons with the calculated sections by FactSage and MTDATA indicated that the oxygen partial pressure has an obvious influence on the molten phase domain and clear deviations from experimental data mainly existed in the primary phase field of rutile. Therefore, the present results are significant for updating the current TiO_x-containing thermodynamic databases, giving a deeper understanding of the related high temperature processes.

Keywords: thermodynamic, equilibrium, ilmenite, titanomagnetite, smelting reduction

1 Introduction

Metallic titanium and its oxide, TiO_2, are widely used in different areas, for instance bone implants, white pigment in paints, automobiles, even nuclear submarines and spacecraft[1]. The crustal abundance of Ti is 0.62 wt%[2], and it mainly coexists with other elements such as Fe, Cr, Mn, Si, etc. in rutile (95 - 100 wt% TiO_2), ilmenite (45 - 53 wt% TiO_2), and titanomagnetite (0 - 34 wt% TiO_2) ores[3]. During the smelting reduction of the ores in a blast furnace or electric furnace, Ti oxides are mainly deported into the slag phase due to their higher stability compared to Fe oxides in reducing conditions[4], and Ti-bearing slags are produced with different concentrations of TiO_x (5-25 wt% for blast furnaces, 45-60 wt% for electric furnaces)[5]. In order to increase the metal extraction efficiencies, as well as the recovery of the enormous Ti resource in slags, the physicochemical properties of TiO_x-containing oxide systems including viscosity[6], structure[7], and crystallization[8] should be systematically investigated. Equilibrium phase relations and liquidus information can be used as the fundamental data to explain the variety of the abovementioned physicochemical properties, and therefore should have the highest priority in experimental studies.

Many metals, such as Fe, Ti, V, Mg, Al, and Cr, are involved in blast and electric furnace smelting reactions. Therefore, an extremely complicated oxide system, described as the $CaO-MgO-CrO_x-FeO_x-VO_x-Al_2O_3-SiO_2-TiO_x$ system, is present in the processes[9]. Considering the solid solutions and the influence of oxygen partial pressure on the oxidation states of the transition metals Fe, Ti, Cr, and V, the difficulty for fundamental studies on this oxide system is increased by several degrees of magnitude. Therefore, the most basic and important $CaO-SiO_2-TiO_x$ system was selected as the focus for long-term research, which will lay the foundation for studies of the higher order or more complicated systems, e.g.,

$CaO\text{-}SiO_2\text{-}MgO\text{-}Al_2O_3\text{-}TiO_x$[10, 11], $CaO\text{-}SiO_2\text{-}TiO_x\text{-}Fe_tO$[12], and $TiO_x\text{-}Fe_tO\text{-}V_yO$[13].

The phase diagrams for the binary sub-systems of $CaO\text{-}SiO_2$[14], $CaO\text{-}TiO_2$[15], and the quasi-binaries of $SiO_2\text{-}TiO_x$[16] have been extensively investigated during the past decades. For the $CaO\text{-}SiO_2\text{-}TiO_x$ ternary system, studies have been mainly conducted in oxidizing atmospheres. In 1955, DeVries *et al.*[17] were the first to systematically study this system in air. They constructed the primary crystal phase fields, e.g., perovskite, rutile, and silica for the $CaO\text{-}SiO_2\text{-}TiO_2$ section with the 1400° C to 1900 °C isotherms. The system was also characterized by a wide immiscibility area. To find the effects of TiO_2 on the sintering of periclase-spinel mixtures, the quasi-binary $CaO{\cdot}TiO_2\text{-}2CaO{\cdot}SiO_2$ system was investigated by Panek *et al.,*[18] focusing on compositions near the eutectic point, and the solution of $CaO{\cdot}TiO_2$ in the $2CaO{\cdot}SiO_2$ phase was found to reach a maximum of 3.61 wt% by X-ray microprobe analysis. Later in 1998, Kirschen *et al.*[19, 20, 21] updated the primary crystal phase fields and immiscibility domain using both equilibrium experiments at 1600 °C and calculations by Kohler extrapolation. Major discrepancies were found in the stability of wollastonite compared with the results by DeVries *et al.*[17]. The quasi-binary systems of $CaO{\cdot}SiO_2\text{-}CaO{\cdot}SiO_2{\cdot}TiO_2$, $CaO{\cdot}SiO_2\text{-}CaO{\cdot}TiO_2$, $CaO{\cdot}SiO_2{\cdot}TiO_2\text{-}TiO_2$, $CaO{\cdot}SiO_2{\cdot}TiO_2\text{-}CaO{\cdot}TiO_2$, $2CaO{\cdot}SiO_2\text{-}CaO{\cdot}TiO_2$, as well as the $CaO\text{-}SiO_2\text{-}TiO_2$ system were optimized by Danek *et al.*[22, 23] with an adapted LeChâtelier-Shreder equation. However, a significant deviation existed in the SiO_2-rich region due to the lack of thermodynamic data for the simulation of the liquid state miscibility gap. In reducing atmospheres, the 1300 °C subsolidus of the $Ti_2O_3\text{-}SiO_2\text{-}CaO$ system was studied by Ye *et al.*[24], and a ternary phase of $3CaO{\cdot}Ti_2O_3{\cdot}3SiO_2$ was detected in a non-oxidizing atmosphere. In a study by Muan *et al.,*[25] a phase diagram of the $CaO\text{-}SiO_2\text{-}Ti_2O_3$ system was constructed for the equilibrium phase relations of transition metal oxides at high temperatures from 1400 °C to 1700 °C and at low oxygen partial pressures of 10^{-10} - 10^{-13} atm. The ternary garnet $3CaO{\cdot}Ti_2O_3{\cdot}3SiO_2$ phase was found to replace the sphene $CaO{\cdot}SiO_2{\cdot}TiO_2$ phase, which is stable in air. The results indicated a significant influence of oxygen partial pressure on the equilibrium phase assemblies.

The precise prediction of the properties of oxide systems at high temperatures requires quantitative knowledge of the thermodynamic data. The equilibrium phase relations of Ti, Fe, V, and Cr need to be extensively investigated under different oxygen partial pressures of industrial interest. In the present work, the $CaO\text{-}SiO_2\text{-}TiO_x$ system was selected to enrich the fundamental studies at 1400 °C at the oxygen partial pressure of 10^{-10} atm. Comparisons of the experimental results were conducted with predictions by FactSage and MTDATA, as well as earlier results from the literature, in order to evaluate the need for updating the current thermodynamic oxide databases.

2 Experimental

High purity oxide powders of CaO (99.99 wt%), SiO_2 (99.99 wt%), and TiO_2 (99.98 wt%) from Sigma-Aldrich were used as starting materials for the experiments. For each sample, 0.15 g of the

oxide mixture was accurately weighed with the pre-set ratios of the components (Table 1), then pressed into cylindrical shape and stored in a desiccator for the equilibrium experiments.

The high temperature equilibrium - quenching technique was employed to determine the phase relations and the 1400 °C isotherm for the CaO-SiO_2-TiO_x system under a reducing atmosphere. The experimental details have been described in our previous publications [10, 11, 26]. A platinum foil was used for supporting the small cylindrical sample pellet, which was then suspended by a platinum wire inside the furnace work tube. Preliminary experiments with extended lead times of 12–48 h proved that 24 h was sufficient to reach equilibrium [26]. Therefore, each sample was equilibrated for at least 24 h to ensure that equilibrium state was reached. Before the platinum foil – sample assembly was pulled up to the hot zone of the furnace, the bottom of the tube was sealed and a reducing CO_2/CO gas mixture was introduced into the tube for at least 30 min to replace the residual air, and to generate the required oxygen partial pressure. After the stabilization, the foils were pulled up to the hot zone for the equilibrium experiments.

After equilibration, the bottom of the tube was opened in the protection of an ice-water bath, and the platinum foil containing the sample was dropped and quenched in the ice water. The quenching process was finished within seconds in order to retain the high temperature phase assemblies and the phase compositions at room temperature.

The quenched samples were dried, mounted in epoxy resin, polished, and coated with carbon for further analysis. A MIRA 3 Scanning Electron Microscope (SEM; Tescan, Brno, Czech Republic) equipped with an UltraDry silicon drift energy dispersive X-ray spectrometer and NSS microanalysis software (EDS; Thermo Fisher Scientific, Waltham, MA, USA) was used to characterize the phase assemblies and compositions of the samples. The following parameters were employed: an accelerating voltage of 15 kV and a beam current of 10 nA on the sample surface. The Proza (Phi-Rho-Z) matrix correction procedure was used for processing the raw data[27]. The external standards utilized in the EDS analyses were anhydrite (for Ca, K), quartz (for O, K and Si, K), and Ti metal (for Ti, K). The mineral and metal microanalysis standards were supplied by Astimex (Toronto, Canada). At least six analysis points were randomly selected from each phase for statistical reliability.

3 Results

3.1 Oxidation state of Ti oxides

During the smelting reduction process of Ti-containing ores, the reducing atmosphere is mainly controlled by the reactions between C, CO, and CO_2, as explained by equations (1) - (3). According to the Ellingham diagram in Figure 1, calculated by HSC Chemistry 9.0[28], Fe oxides can be reduced step-by-step by CO or C from Fe_2O_3 to Fe_3O_4, then to FeO, and finally to metallic Fe at blast furnace smelting temperatures[29, 30]. Simultaneously, V and Cr oxides can also be reduced to metallic state. In contrast, Ti oxides such as TiO_2, Ti_2O_3, and TiO in the ores are

difficult to reduce. The different oxide stability refers to the C/CO/CO_2 reactions eventually lead to the production of a metallic Fe-V-Cr-C alloy and a TiO_x-rich slag.

$$2C\ (s) + O_2\ (g) = 2CO\ (g)\ \Delta G^{\theta}\ (kJ{\cdot}mol^{-1}) = -274.02 - 0.17\ T\ (°C)^{[28]} \quad (1)$$

$$C\ (s) + O_2\ (g) = CO_2\ (g)\ \Delta G^{\theta}\ (kJ{\cdot}mol^{-1}) = -395.18 - 0.0007\ T\ (°C)^{[28]} \quad (2)$$

$$2CO\ (g) + O_2\ (g) = 2CO_2\ (g)\ \Delta G^{\theta}\ (kJ{\cdot}mol^{-1}) = -516.34 + 0.17\ T\ (°C)^{[28]} \quad (3)$$

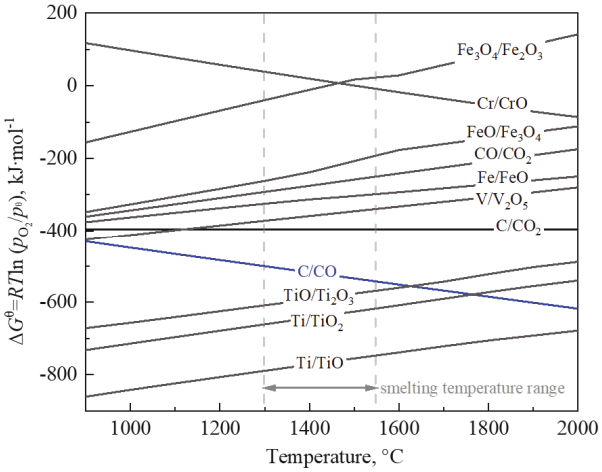

No.	Reactions	ΔG^{θ} (kJ·mol^{-1})=A+B*T(°C) (200 – 2000 °C)	
		A, kJ·mol^{-1}	B, kJ·mol^{-1}·°C^{-1}
1	$2C\ (s)+ O_2(g) = 2CO(g)$	-274.02	-0.17
2	$C\ (s)+ O_2(g) = CO_2(g)$	-395.18	-0.0007
3	$2CO\ (g) + O_2(g) = 2CO_2(g)$	- 516.34	0.17
4	$2Fe\ (s) + O_2(g) = 2FeO\ (s)$	- 485.55	0.12
5	$6FeO\ (s)+ O_2(g) = 2Fe_3O_4\ (s)$	- 550.78	0.23
6	$4Fe_3O_4\ (s) + O_2(g) = 6Fe_2O_3\ (s)$	- 411.87	0.28
7	$2Ti\ (s)+ O_2(g) = 2TiO\ (s)$	- 1022	0.18
8	$4TiO\ (s)+ O_2(g) = 2Ti_2O_3\ (s)$	- 815.02	0.16
9	$Ti\ (s) + O_2(g) = TiO_2\ (s)$	- 891.57	0.18
10	$4/5V\ (s)+ O_2(g) = 2/5V_2O_5\ (s)$	- 556.06	0.14
11	$2Cr\ (s) + O_2(g) = 2CrO(g)$	298.1	-0.20

Figure 1. The Ellingham diagram for selected reduction reactions involving metallic elements Fe, Ti, V, and Cr.

In order to reveal the oxidation states of Ti oxides in the slag at different oxygen partial pressures and temperatures, a predominance phase diagram of the Ti - O system was plotted by FactSage 7.3[31], as shown in Figure 2. In blast furnace smelting temperature ranges[29], TiO_2 can be reduced to lower valence oxides, Ti_3O_5, Ti_2O_3, and TiO, along with continuously decreasing oxygen partial pressure. The Magnéli phases with a general formula of Ti_nO_{2n-1} ($n \geq 4$) can also be formed before the formation of Ti_3O_5. In the present work, an experimental oxygen partial pressure of 10^{-10} atm, 1 atm total pressure, and a temperature of 1400 °C were selected as global constraints to investigate the equilibrium phase relations of the CaO-SiO_2-TiO_x system.

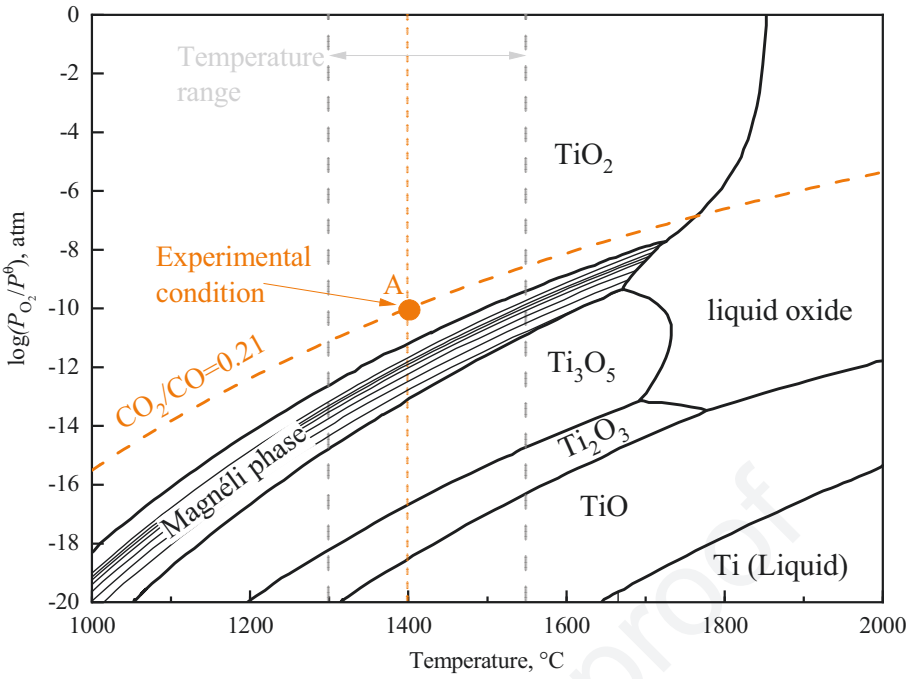

Figure 2. Stable regions of Ti oxides as functions of T and $\log(P_{O_2}/P^{\Theta})$ in the Ti-O_2 system. The lines between the TiO_2 and Ti_3O_5 regions are the phase boundaries of several Magnéli phases with the formula of Ti_nO_{2n-1} ($n \geq 4$)

The Boudouard reaction (3) controlled the oxygen partial pressure by the CO/CO_2 gas mixture during the equilibration process. The prevailing oxygen partial pressure could be calculated by equation (4), where delta G (J·mol^{-1}) is the standard Gibbs energy of reaction (3), R is the gas constant with a value of 8.314 (J·mol^{-1}·K^{-1}), T is the temperature in K, P^{θ} is the standard atmospheric pressure (1 bar), while P_{CO_2}, P_{CO}, P_{O_2} are the partial pressures for CO_2, CO, and O_2, respectively. In order to realize the experimental condition of $P_{O_2} = 10^{-10}$ atm at 1400 °C, a total flow rate of 300 mL/min with a volumetric CO_2/CO ratio of 0.21 was used. The experimental P_{O_2} and T was also projected on Figure 2 with label A. According to the above calculation, the stable form of pure titanium oxides during the experiments was TiO_2, and therefore this oxidation state was adopted for the discussion in the following sections.

$$\log\left(\frac{P_{O_2}}{P^{\Theta}}\right) = 0.434\frac{\Delta G^{\theta}}{RT} + 2\log\frac{P_{CO_2}}{P_{CO}} \quad (4)$$

3.2 Equilibrium phases at oxygen partial pressure of 10^{-10} atm and 1400 °C

The microstructures of the equilibrium phases are presented in Figures 3(a) to 3(f), while the corresponding phase compositions are listed in Table 1. In total, four two-phase equilibrium assemblies were found. A liquid-silica equilibrium was confirmed in the high SiO_2 domain and was represented by sample #1 in Figure 3(a) with light gray and dark gray phases, respectively. When the CaO concentration in the sample increased from base sample #1, a liquid-wollastonite equilibrium was detected, as shown by sample #5 in Figure 3(b). Furthermore, liquid-perovskite and liquid-rutile equilibrium assemblies could be identified as the TiO_2 concentration in the

samples kept increasing, as shown in Figures 3(c) and 3(d) by samples #7 and #10, respectively.

Moreover, a three-phase equilibrium of condensed phases (liquid-silica-rutile) was confirmed in samples #12, #13, #14, as shown in Figure 3(e) with the medium gray (liquid), dark gray (silica), and light gray (rutile) phases displayed by sample #13. According to the Gibbs phase rule[32], the degrees of freedom *f* in a system can be expressed with the following equation (5):

$$f = (S - R - Z) - P + 2 = C - P + 2 \quad (5)$$

where *S* is the total number of components in the system, *R* is the number of independent chemical reactions, *Z* is the number of constraints, *C* is the number of independent components, and *P* is the number of coexisting phases, while 2 stands for the environmental conditions of temperature and total pressure.

For the equilibrium process of the CaO-SiO_2-TiO_x system involving gases under partial pressure of $P_{O_2} = 10^{-10}$ atm at 1400 °C, TiO_x existed as TiO_2 according to the predominance phase diagram in Figure 2. Therefore, the total components were CaO, SiO_2, TiO_2, CO, CO_2, C, and O_2, thus $S = 7$. Meanwhile, there were 2 independent chemical reactions between equations (1) to (3), and thus $R = 2$. In addition, there was one concentration constraint with a fixed CO_2/CO ratio of 0.21 (or oxygen partial pressure), and thus $Z = 1$. Therefore, the number of independent components is $C = S - R - Z = 7 - 2 - 1 = 4$. Moreover, as gas was involved in the equilibrium process, the number of coexisting phases *P* is 4 for samples #12, #13, and #14 between the gas and the condensed three-phase equilibrium of liquid-silica-rutile. Furthermore, when the environmental parameters of temperature and total pressure were fixed at 1400 °C and 1 atm, the degrees of freedom *f* for the liquid-silica-rutile-gas equilibrium could finally be confirmed as $f = C - P = 4 - 4 = 0$. This means that the composition of the coexisting liquid oxide forms a constrained invariant point in the CaO-SiO_2-TiO_x system. The composition of the invariant point can be thus calculated as the average of samples #12, #13, and #14, which yields 54.7 wt% TiO_2 + 24.6 wt% SiO_2 + 20.7 wt% CaO.

The single-phase equilibrium of liquid, shown in Figure 3(f), was found in a different composition domain in samples #15, #16, and #17, implying that two liquid oxides domains may exist under these experimental conditions. Normally, the compositions of a single liquid phase cannot be used for constructing the isotherm directly. It may still be quite useful, however, in judging whether the constructed isotherm is right or not. This will be discussed in the following paragraphs.

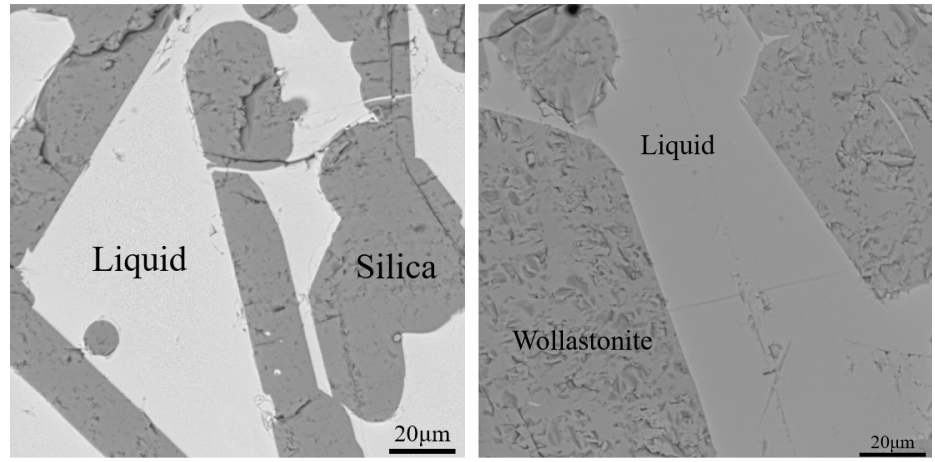

(a) #1 (b) #5

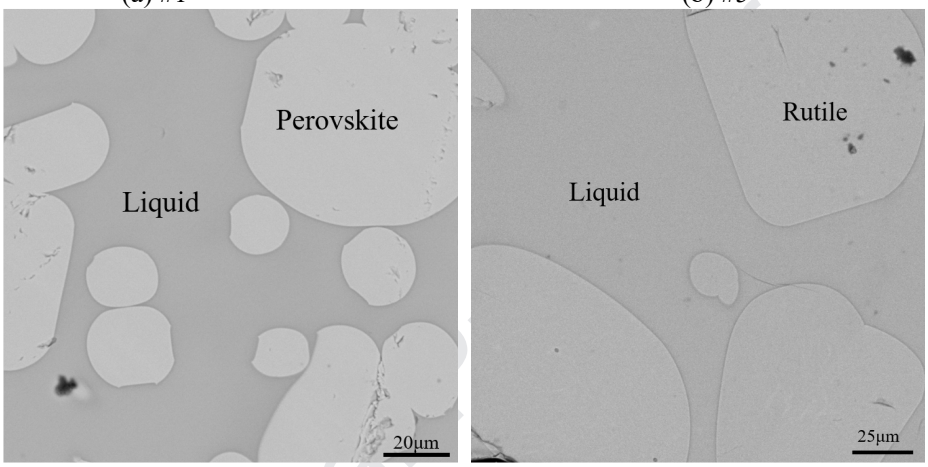

(c) #7 (d) #10

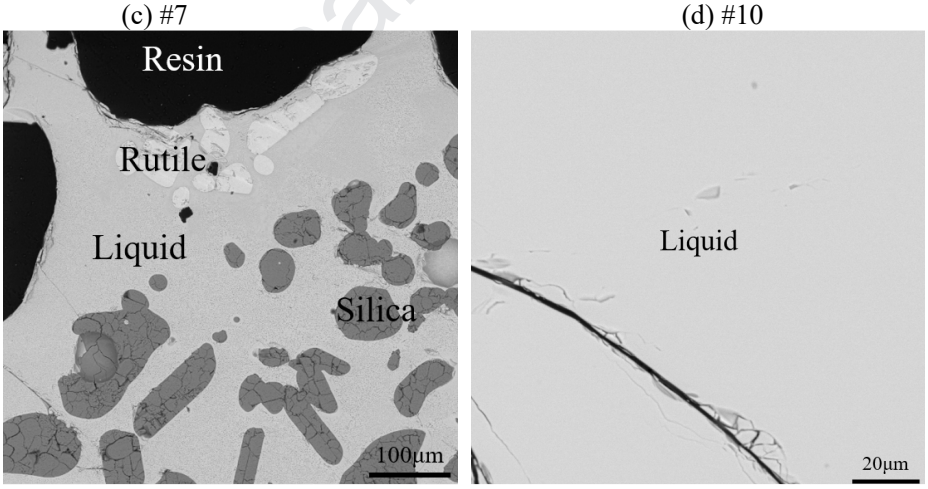

(e) #13 (f) #15, #16, #17

Figure 3. The microstructures of the equilibrium phases at 1400 °C at $P_{O_2} = 10^{-10}$ atm.

Table 1. The compositions of the equilibrium phases at 1400 °C under $P_{O_2} = 10^{-10}$ atm.

No.	Initial composition, wt%			Phases	Equilibrium phase composition, wt%		
	TiO_2	SiO_2	CaO		TiO_2	SiO_2	CaO
#1	12.00	75.00	13.00	Liquid	29.4 ± 0.5	43.2 ± 1.2	27.4 ± 0.9
				Silica	1.6 ± 0.4	98.3 ± 0.6	0.1 ± 0.2
#2	8.00	72.00	20.00	Liquid	15.7 ± 1.2	52.8 ± 0.8	31.5 ± 0.4
				Silica	1.0 ± 0.5	99.0 ± 0.5	0.0
#3	2.00	65.00	33.00	Liquid	14.4 ± 0.9	55.5 ± 1.4	30.1 ±0.7
				Silica	0.8 ± 0.3	98.9 ± 0.9	0.3 ± 0.6
#4	10.00	45.00	45.00	Liquid	14.3 ± 0.2	46.5 ± 0.2	39.2 ± 0.1
				Wollastonite	0.4 ± 0.1	50.1 ± 0.3	49.5 ± 0.3

#5	5.00	42.00	53.00	Liquid	14.8 ± 0.6	37.3 ± 0.5	48.0 ± 0.1
				Wollastonite	0.5 ± 0.1	50.0 ± 0.3	49.5 ± 0.3
#6	28.00	28.00	44.00	Liquid	25.9 ± 0.1	35.5 ± 0.1	38.6 ± 0.0(3)
				Perovskite	58.8 ± 0.4	0.1 ± 0.0(2)	41.1 ± 0.4
#7	42.00	22.00	36.00	Liquid	43.5 ± 0.5	25.5 ± 1.1	31.0 ± 0.6
				Perovskite	59.5 ± 0.1	0.1 ± 0.0(2)	40.4 ± 0.1
#8	56.00	12.00	32.00	Liquid	54.9 ± 0.4	19.9 ± 1.1	25.2 ± 0.9
				Perovskite	59.6 ± 0.1	0.1 ± 0.0(3)	40.3 ± 0.1
#9	69.00	5.00	26.00	Liquid	74.0 ± 1.1	5.5 ± 0.9	20.5 ± 0.2
				Perovskite	59.8 ± 0.2	0.1 ± 0.0(1)	40.1 ± 0.2
#10	80.00	7.00	13.00	Liquid	67.0 ± 0.4	11.9 ± 0.1	21.1 ± 0.5
				Rutile	99.5 ± 0.2	0.3 ± 0.0(3)	0.2 ± 0.2
#11	65.00	18.00	17.00	Liquid	58.1 ± 0.5	20.9 ± 0.2	21.0 ± 0.5
				Rutile	99.4 ± 0.1	0.4 ± 0.0(3)	0.2 ± 0.1
#12	50.00	32.00	18.00	Liquid	54.8 ± 2.3	23.9 ± 1.2	21.3 ± 1.3
				Silica	2.9 ± 0.0(4)	97.1 ± 0.0(4)	0.0
				Rutile	99.4 ± 0.1	0.5 ± 0.0(3)	0.1 ± 0.1
#13	40.00	45.00	15.00	Liquid	56.0 ± 0.3	23.5 ± 0.2	20.5 ± 0.1
				Silica	2.6 ± 0.1	97.4 ± 0.1	0.0
				Rutile	99.0 ± 0.1	0.5 ± 0.0(1)	0.5 ± 0.1
#14	30.00	60.00	10.00	Liquid	53.3 ± 1.1	26.3 ± 1.6	20.4 ± 0.6
				Silica	2.8 ± 0.1	97.2± 0.1	0.0
				Rutile	99.4 ± 0.1	0.5 ± 0.1	0.1 ± 0.1
#15	10.00	50.00	40.00	Liquid	13.8 ± 0.1	51.8 ± 0.2	34.4 ± 0.1
#16	8.00	38.00	54.00	Liquid	10.4 ± 0.1	37.7 ± 0.3	51.9 ± 0.2
#17	14.00	32.00	54.00	Liquid	11.6 ± 0.5	38.8 ± 0.1	49.6 ± 0.1

3.3 Construction of the 1400 °C isotherm at $P_{O_2} = 10^{-10}$ atm

Based on the above phase compositions, the 1400 °C isotherm of the system at $P_{O_2} = 10^{-10}$ atm was constructed and projected on the CaO-SiO_2-TiO_x plane in Figure 4. The solid line in Figure 4 is the 1400 °C isotherm based on the equilibrium liquid compositions of this study, while the short-dashed lines are the predicted lines for depicting the invariant points involving the three-phase equilibrium of liquid-rutile-perovskite, liquid-perovskite-wollastonite, and liquid-wollastonite-silica, respectively. In Figure 4, the 1400 °C isotherm in air by DeVries *et al.*[17] was also plotted as a purple dashed line to reveal the influence of the oxygen partial pressure. The liquid phase area was apparently enlarged when the oxygen partial pressure decreased from air to 10^{-10} atm. There is a fair agreement of the liquid compositions for the two-liquid equilibrium of the liquid-silica domain. However, the low oxygen partial pressure of 10^{-10} atm leads to the shrinking of the primary phase areas of wollastonite and rutile, while the primary phase area of perovskite was greatly extended to much higher TiO_2 and lower SiO_2 concentrations, indicating that the lower oxygen partial pressure had an great influence on decreasing the stability of TiO_2, while favorable for the formation of perovskite phase. At the same time, the invariant point for the liquid-rutile-silica equilibrium at $P_{O_2} = 10^{-10}$ atm moved in the direction of slightly higher TiO_2 and lower SiO_2 concentrations.

In Figure 5, the 1400 °C isotherm at $P_{O_2} = 10^{-10}$ atm was calculated by FactSage 7.3[31] with the Equilib module using the FactPS and FToxide databases. The calculated isotherms in the primary phase fields of wollastonite and perovskite agreed well with the present experimental results; however, the calculated liquidus area greatly expanded towards the higher SiO_2

concentration region for the primary phase fields of silica and rutile. It is worth mentioning that FactSage also predicted a second liquid domain in the high CaO content range at $P_{O_2} = 10^{-10}$ atm, which coincides with the present experimental results, as shown by the liquid compositions of samples #16 and #17. However, the experimentally determined liquid compositions of samples #16 and #17 were not located inside this computational liquid area. More experimental data are needed to depict and fit the exact shape of this part of the isothermal section, as in the FactSage databases the molten oxide phase is much too stable in the low CaO regions.

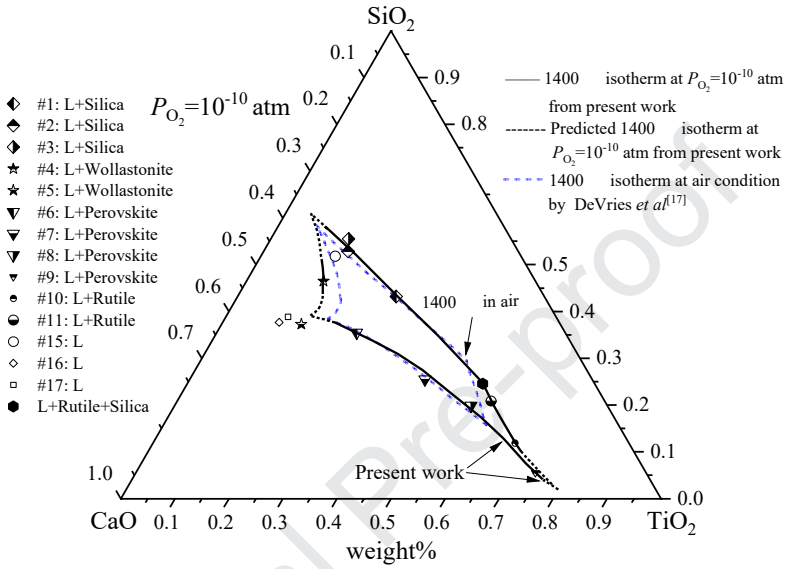

Figure 4. A comparison of the 1400 °C isotherms from the present work and results from DeVries *et al.* [17] .

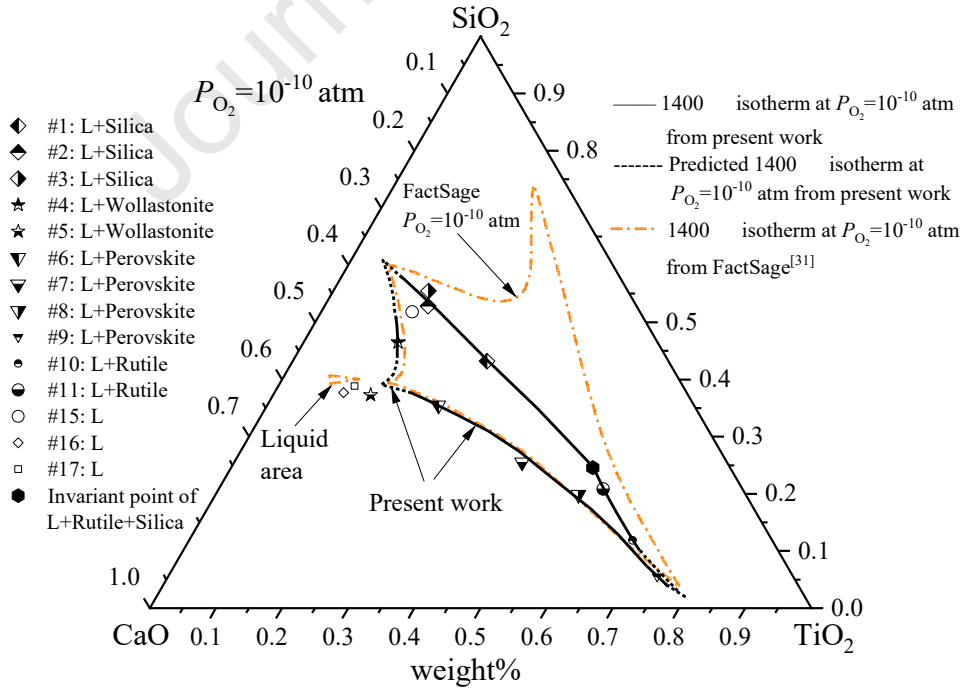

Figure 5. A comparison of the 1400 °C isotherms from the present work and the FactSage prediction.

Similarly, the 1400 °C isotherm at $P_{O_2} = 10^{-10}$ atm was also predicted by MTDATA 8.2[33] with the Mtox and Mtoxsup databases and is shown in Figure 6, where a full assessment of the

CaO-Fe-Ti-O-MgO-Al_2O_3-SiO_2 system is available[34]. The predicted 1400 °C isotherm had a perfect fit with the present experimental results in the primary phase fields of perovskite, rutile, and silica. For wollastonite, the calculation gave a larger primary phase equilibrium area. It seems that the molten oxide phase in the MTDATA databases is slightly less stable than it should be and, therefore, wollastonite extends far from the CaO-SiO_2 binary, i.e., to too high TiO_x concentrations. From the comparisons of experimental results with thermodynamic predictions, it is convinced that the database in MTDATA is more reasonable for TiO_x-containing system regarding to current experimental parameters. The large deviations in FactSage may come from the fact that the database is only developed for reducing conditions when Ti presented, and the liquid phase is generally modeled for binary system, while the ternary and higher-order systems is only estimated from the model due to lack of any experimental data. This strongly affects the FactSage predictions in the Ti-O containing systems. More effort is needed for the update of the Ti oxide containing thermodynamic database of FactSage.

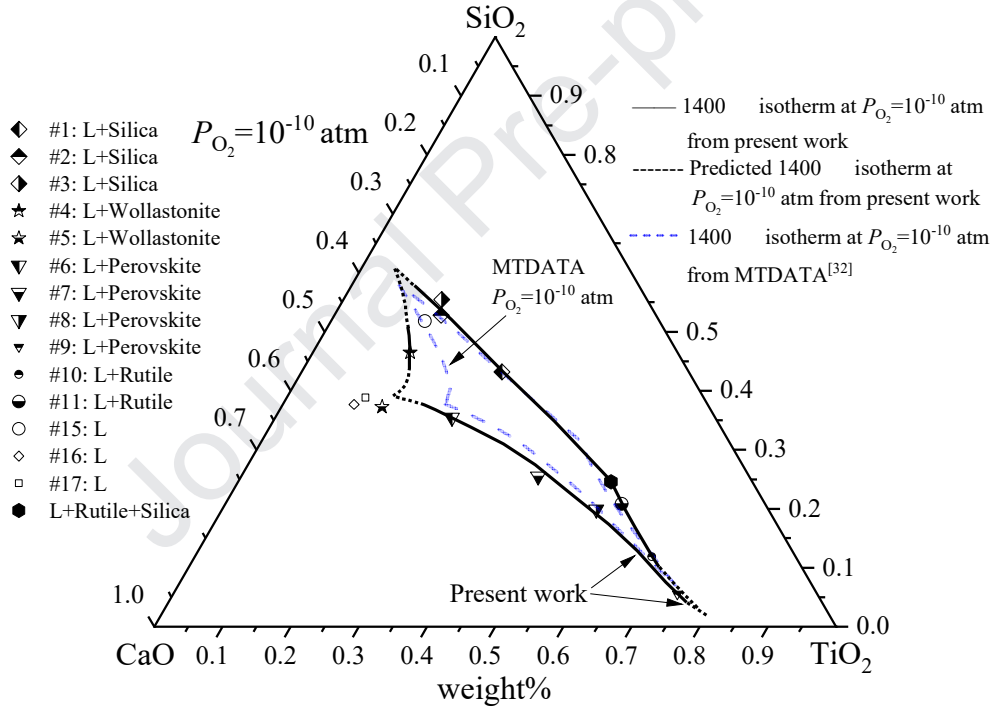

Figure 6. A comparison of the 1400 °C isotherms of the present work and the MTDATA prediction.

4 Conclusions

The CaO-SiO_2-TiO_x system plays an important role in the smelting reduction processes of Ti-containing ores, as well as in the comprehensive recovery of Ti resources from Ti-bearing slags. In the present work, the equilibrium phase relations and the $P_{O_2} = 10^{-10}$ atm isotherm at 1400 °C were experimentally determined using an equilibrium-quenching technique. A comparison of the experimental results between the present work and the literature revealed that lower oxygen partial pressures lead to shrinkage of the rutile and wollastonite primary phase

areas.

In addition, the predictions by FactSage and MTDATA databases were also compared with the experimental results. The observed deviations from the computational diagrams were discussed in detail to indicate key directions for future experiments. The fundamental data obtained from the present work is useful for a better understanding of the reaction sequences taking place in ilmenite and titano-magnetite ores in reducing conditions. Moreover, the data are also important for updating the present thermodynamic databases of high-order, Ti-containing oxide systems.

Acknowledgements

The authors wish to acknowledge the contributions of Aalto University. This study utilized the Academy of Finland's RawMatTERS Finland Infrastructure (RAMI) housed jointly at Aalto University, GTK, and VTT in Espoo.

Disclosure statement

The authors report no conflicts of interest and the authors alone are responsible for the content and writing of the article.

Funding

The study received financial support from Aalto University and the China Scholarship Council.

References

[1]. C. Veiga, J. Davim, A. Loureiro, Properties and applications of titanium alloys: a brief review, Rev. Adv. Mater. Sci. 32(2) (2012) 133-148.

[2]. K.H. Wedepohl, The composition of the continental crust, Geochim. Cosmochim. Acta 59(7) (1995) 1217-1232.

[3]. A. Dehghan-Manshadi, J. Manuel, S. Hapugoda, N. Ware, Sintering characteristics of titanium containing iron ores, ISIJ Int. 54(10) (2014) 2189-2195, https://doi.org/10.2355/isijinternational.54.2189.

[4]. P. Stratton, Ellingham diagrams–their use and misuse, Int. Heat Treat. Surf. Eng. 7(2) (2013) 70-73, https://doi.org/10.1179/1749514813Z.00000000053.

[5]. Z. Wang, Q. Zhu, H. Sun, Phase Equilibria in the TiO_2-Rich Part of the TiO_2-CaO-SiO_2-10 Wt Pct Al_2O_3-5 Wt Pct MgO System at 1773 K, Metall. Mater. Trans. B 50(1) (2019) 357-366, https://doi.org/10.1007/s11663-018-1441-2.

[6]. C. Feng, J. Tang, L. Gao, Z. Liu, M. Chu, Effects of CaO/SiO_2 on Viscous Behaviors and Structure of CaO-SiO_2-11.00 wt% MgO-11.00 wt% Al_2O_3-43.00 wt% TiO_2 Slag Systems, ISIJ Int. 59(1) (2019) 31-38, https://doi.org/10.2355/isijinternational.ISIJINT-2018-444.

[7]. K. Zheng, J. Liao, X. Wang, Z. Zhang, Raman spectroscopic study of the structural properties of CaO-MgO-SiO_2-TiO_2 slags, J. Non-Cryst. Solids. 376 (2013) 209-215, https://doi.org/10.1016/j.jnoncrysol.2013.06.003.

[8]. Q. Zhao, C. Liu, L. Cao, M. Jiang, B. Li, H. Saxén, R. Zevenhoven, Shear-force based

stainless steel slag modification for chromium immobilization, ISIJ Int. 3 (2019) 583-589, https://doi.org/10.2355/isijinternational.ISIJINT-2017-678.

[9]. I.-H. Jung, Overview of the applications of thermodynamic databases to steelmaking processes, Calphad 34(3) (2010) 332-362, https://doi.org/10.1016/j.calphad.2010.06.003.

[10]. J. Shi, M. Chen, I. Santoso, L. Sun, M. Jiang, P. Taskinen, A. Jokilaakso, 1250° C liquidus for the CaO-MgO-SiO_2-Al_2O_3-TiO_2 system in air, Ceram. Int. 46(2) (2020) 1545-1550, https://doi.org/10.1016/j.ceramint.2019.09.122.

[11]. L. Sun, J. Shi, C. Liu, M. Jiang, Phase equilibria studies for CaO-SiO_2-5wt.% MgO-Al_2O_3-TiO_2 system in high Al_2O_3 content area with w(CaO)/w(SiO_2) ratio of 1.50, J. Alloys Compd. 810 (2019) 151949, https://doi.org/10.1016/j.jallcom.2019.151949.

[12]. D. Xirouchakis, D.H. Lindsley, Equilibria among titanite, hedenbergite, fayalite, quartz, ilmenite, and magnetite: experiments and internally consistent thermodynamic data for titanite, Am. Mineral. 83(7-8) (1998) 712-725, https://doi.org/10.2138/am-1998-7-804.

[13]. T. Coetsee, High temperature phase relations in the TiO_x-FeO_y-VO_z system, PhD thesis, University of Pretoria, South Africa, 2006.

[14]. G. Eriksson, P. Wu, M. Blander, A.D. Pelton, Critical evaluation and optimization of the thermodynamic properties and phase diagrams of the MnO-SiO_2 and CaO-SiO_2 systems, Can. Metall. Q. 33(1) (1994) 13-21, https://doi.org/10.1179/cmq.1994.33.1.13.

[15]. K. Jacob, S. Gupta, Phase diagram of the system Ca-Ti-O at 1200 K, Bull. Mater. Sci. 32(6) (2009) 611-616, https://doi.org/10.1007/s12034-009-0094-9.

[16]. J.I. Goldstein, S.K. Choi, F.J. Van Loo, G.F. Bastin, R. Metselaar, Solid state Reactions and Phase Relations in the Ti Si O System at 1373 K, J. Am. Ceram. Soc. 78(2) (1995) 313-322, https://doi.org/10.1111/j.1151-2916.1995.tb08802.x.

[17]. R. DeVries, R. Roy, E. Osborn, Phase Equilibria in the System CaO-TiO_2-SiO_2, J. Am. Ceram. Soc. 38(5) (1955) 158-171, https://doi.org/10.1111/j.1151-2916.1955.tb14922.x.

[18]. Z. Panek, The effect of TiO_2 on phase transformations of periclase-spinellitic systems in the presence of silicates, Ceram.-Silik. 20(1) (1976) 13-22.

[19]. M. Kirschen, C. DeCapitani, "Immiscible Liquids in the MgO-CaO-SiO_2-Al_2O_3-TiO_2 System"; pp. 2537-2542 in Proc. Int. Congr. Glass, 18th (Computer Optical Disk), San Francisco, California, July 5-10, 1998. Edited by M. K. Choudhary, The American Ceramic Society, Westerville, Ohio, 1998.

[20]. C. DeCapitani, M. Kirschen, A generalized multicomponent excess function with application to immiscible liquids in the system CaO-SiO_2-TiO_2, Geochim. Cosmochim. Acta 62(23-24) (1998) 3753-3763, https://doi.org/10.1016/S0016-7037(98)00319-6.

[21]. M. Kirschen, C. De Capitani, Immiscible silicate liquids in the CaO-SiO_2-TiO_2-Al2O_3 system,

Schweiz. Mineral. Petrogr. Mitt. 78(1) (1998) 175-178.

[22]. V. Dan k, I. Nerád, Phase Diagram and Structure of Melts of the System CaO-TiO_2-SiO_2, Chem. Pap. 56(4) (2002) 241-246.

[23]. I. Nerad, V. Danek, Thermodynamic Analysis of Pseudobinary Subsystems of the System CaO-TiO_2-SiO_2, Chem. Pap. 56(2) (2002) 77-83.

[24]. G. Ye, T. Rosenqvist, Phase relations in the Ti-Si-Ca-O system under reducing conditions, and silicothermic reduction of titanium oxide, Scand. J. Metall. 20(4) (1991) 222-228.

[25]. A. Muan, Equilibrium Relations Involving Transition-Metal Oxides at High Temperatures, Adv. Ceram. III, Springer,1990, pp. 25-44.

[26]. M. Chen, J. Shi, P. Taskinen, A. Jokilaakso, Experimental determination of the 1300° C and 1400° C isotherms for CaO–SiO_2–TiO_2-10 wt% Al_2O_3 system in air, Ceram. Int. 46(7) (2020) 9183-9191, https://doi.org/10.1016/j.ceramint.2019.12.170.

[27]. G. Bastin, H. Heijligers, Quantitative electron probe microanalysis of ultra-light elements (boron-oxygen), Electron Probe Quant. Springer1991, pp. 145-161.

[28]. A. Roine, HSC Chemistry for Windows, vers. 9.2.6 (Pori, Finland: Outotec Research, 2019). www.hsc-chemistry.com. Accessed 25 June 2019.

[29]. P. Pistorius, Ilmenite smelting: the basics, J. South. Afr. Inst. Min. Metall. 108(1) (2008) 35-43.

[30]. Miaoyong Zhu. Modern ferrous metallurgy. Beijing: Metallurgical Industry Press Co., Ltd, 2005.

[31]. C. Bale, E. Bélisle, P. Chartrand, S. Decterov, G. Eriksson, K. Hack, I.-H. Jung, Y.-B. Kang, J. Melançon, A. Pelton, FactSage thermochemical software and databases-recent developments, Calphad 33(2) (2009) 295-311, https://doi.org/10.1016/j.calphad.2008.09.009.

[32]. M.Y. Zhao, L.Z. Song, X.B. Fan. The boundary theory of phase diagrams and its application. Beijing: Science Press, 2009.

[33]. R. Davies, A. Dinsdale, J. Gisby, J. Robinson, A. M. Martin, MTDATA- thermodynamic and phase equilibrium software from the national physical laboratory, Calphad 26(2) (2002) 229-271.

[34]. J. Gisby, P. Taskinen, J. Pihlasalo, Z. Li, M. Tyrer, J. Pearce, K. Avarmaa, P. Björklund, H. Davies, M. Korpi, MTDATA and the prediction of phase equilibria in oxide systems: 30 years of industrial collaboration, Metall. Mater. Trans. B 48(1) (2017) 91-98, https://doi.org/10.1007/s11663-016-0811-x.

(1) Equilibrium phase relations were experimental determined for CaO-SiO_2-TiO_x system at 1400 °C under oxygen partial pressure of 10^{-10} atm.
(2) Equilibria phases of perovskite, wollastonite, rutile, and silica were found to coexist with liquid oxide.
(3) The 1400 °C isotherm was constructed and compared with thermodynamic software predictions.
(4) Lower oxygen partial pressures led to shrinkage of the rutile and wollastonite primary phase fields.

The authors declare that they have no known competing financial interests or personal relationships that could have appeared to influence the work reported in this paper.